ISSN 1726-5479

SENSORS & TRANSDUCERS

11/08 vol. 98

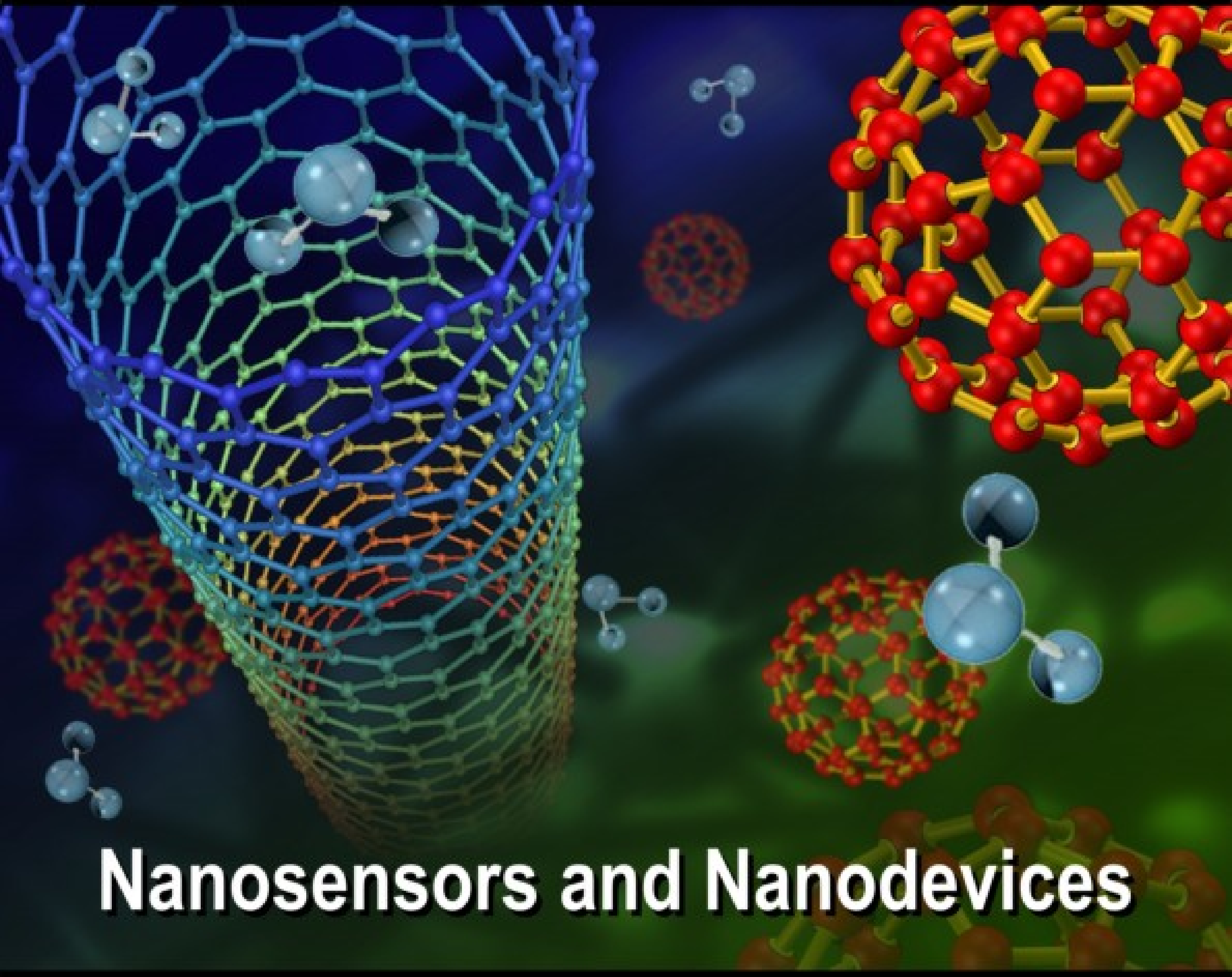

Nanosensors and Nanodevices

International Frequency Sensor Association Publishing

IFSA

Sensors & Transducers

Volume 98
Issue 11
November 2008

www.sensorsportal.com

ISSN 1726-5479

Sensors & Transducers Journal (ISSN 1726-5479) is a peer review international journal published monthly online by International Frequency Sensor Association (IFSA).
Available in electronic and CD-ROM.

Sensors & Transducers Journal

Contents

Volume 98
Issue 11
November 2008

www.sensorsportal.com

ISSN 1726-5479

Research Articles

Nanotechnology-Enabled Sensors: Book Review
S.Y. Yurish………………………………………………………………………………………………….. I

Room Temperature Ammonium Gas Sensing Behavior of Upright-standing ZnO Nano-sheets
Arindam Ghosh , Yuvraj G. Gudage, Ramphal Sharma, Rajaram S. Mane and Sung-Hwan Han 1

Synthesis of Nanocrystalline SnO2 Modified TiO2: a Material for Carbon Monoxide Gas Sensor
A. B. Bodade, M. Alvi, A. V.Kadu, S. V.Jagtap, S. K. Rithe, P. R. Padole and G. N. Chaudhari 6

Glucose Biosensor Based on Electrostatically Functionalized Carbon Nanotubes Bound Glucose Oxidase
Suman, Ashok Kumar, V. K. Jain 16

CO Sensing Properties of Nanostructured $La_{0.8}Sr_{0.2}CoO_3$ Sensors Synthesized by EDTA-Glycol Method
G. N. Chaudhari, A. B. Bodade, S. V. Jagatap, M. J. Pawar 26

Pt/GaN Schottky Diode for Propene (C3H6) Gas Sensing
M. Shafiei, K. Kalantar-Zadeh, M. Kocan, G. Parish, J. Antoszewski, L. Faraone, W. Wlodarski 38

All-digital PLL System for Self-oscillation Mode of Microcantilevers with Integrated Bimorph Actuator and Piezoresistive Readout
Nikolay Nikolov, Nikolay Kenarov, Peycho Popov, Theodor Gotszalk, Ivo Rangelow....................... 45

Modelling of Spring Constant and Pull-down Voltage of Non-uniform RF MEMS Cantilever Incorporating Stress Gradient
Shimul Chandra Saha, Ulrik Hanke, Geir Uri Jensen, Trond Sæther 54

Analysis of a Bimorph Accelerometer Using Analytical and Finite Element Modeling
Hou Xiaoyan. 69

Design of a High Performance MEMS Pressure Sensor Array with Signal Conditioning Unit for Oceanographic Applications
C. RoyChaudhuri, V. Natarajan, P. Chatterjee, S. Gangopadhyay, V. Sreeramamurthy, H. Saha ... 83

On the Modeling of an Open Channel MEMS Based Capacitive Flow Sensor
Vafaghi Maryam, Besharat Sina, Rezazadeh Ghader, Motallebi Asadollah...................................... 96

Authors are encouraged to submit article in MS Word (doc) and Acrobat (pdf) formats by e-mail: editor@sensorsportal.com
Please visit journal's webpage with preparation instructions: http://www.sensorsportal.com/HTML/DIGEST/Submition.htm

International Frequency Sensor Association (IFSA).

Sensors & Transducers Journal, Vol. 98, Issue 11, November 2008, pp. 69-82

www.sensorsportal.com

Sensors & Transducers

ISSN 1726-5479

http://www.sensorsportal.com

Analysis of a Bimorph Accelerometer Using Analytical and Finite Element Modeling

Hou Xiaoyan
Department of Civil Engineering, National University of Singapore
Singapore 117576
Email: houxiaoyan@gmail.com

Received: 19 August 2008 /Accepted: 17 November 2008 /Published: 30 November 2008

Abstract: In this paper, a Bimorph Accelerometer with symmetric bimorphs and central supporting pole configuration is developed and analytically characterized. Calibration function is defined to describe the system dynamics of the accelerometer. Closed-form expression for the calibration function is then derived based on piezoelectric constitutive equations and beam theory. The analysis takes into account the effect of device geometry and material properties, and agrees well with the results obtained by the finite element analysis. Besides producing accurate predications, it is found that with appropriate geometrical dimensions, both high sensitivity and broad frequency bandwidth, two most important parameters in evaluating accelerometers, can be achieved. *Copyright © 2008 IFSA.*

Keywords: Piezoelectric bimorph, Accelerometer, Translational DOF, Frequency bandwidth

1. Introduction

The piezoelectric bimorph is an invention by C. Baldwin Sawyer in 1931 [1-3]. In a bimorph, two piezoelectric patches are bonded together. A center metal shim is often laminated between the two piezoelectric patches to add mechanical strength and stiffness. A bimorph element usually also has four electrode layers and two adhesive layers, since these layers are much thinner than the PZT and metal layers, their effect is normally neglected in analysis [1].

Bending bimorphs possess high motion and voltage sensitivity [2]. They are widely used as electromechanical transducers such as positioners [4], laser beam deflectors [5-6], air acoustic transducers [7], loudspeakers [8], pumps and valves [9], ultrasonic motors [10], numerical displays

[11], etc. As bimorphs can effectively convert mechanical energy to electrical energy, they also function well as accelerometers, though not so popular [12].

In 1989, a novel bimorph accelerometer has both translational and rotational sensing capability was proposed by Bill and Wicks and later developed into commercial products by Kistler [12-13]. This accelerometer is one of the few commercially available accelerometers that can measure rotational motion. It can also get translational motion simultaneously. In their work, Bill *et al.* related the output charge of the accelerometer with the mass, length and thickness of the bimorph and the piezoelectric constant of the PZT materials. Their model is highly simplified. The influence of some important geometric and material properties of bimorph including width, dielectric constant and stiffness constant was not included in their analysis. In addition, the working frequency range of the accelerometer is up to only 2000 Hz, which is too low for mini-structures whose interested frequency range sometimes up to tens of thousands hertz.

When bimorph is used as a sensor, a bending or deflection of the bimorph places one PZT patch in tension and the other patch in compression. As a result of the induced stresses, the bimorph generates an electrical output signal due to the direct piezoelectric effect. As a sensor, the bimorph has the advantage of detecting even small mechanical deformation. Bimorphs also have other advantages including low cost, simple structure, easy integration with electronic circuitry, and high sensitivity, which made them ideal for accelerometers. It is therefore necessary to develop more bimorph-based accelerometers for various dynamic applications.

In the past decades, a lot of researchers have tried to analytically model bending bimorphs. A significant amount of scientific literature has been published in this area [e.g. 14-18]. The two most widely used approaches are admittance matrix approach and equivalent circuit approach.

Admittance matrix approach is extensively adopted in modeling bimorph transducers as it describes the electromechanical coupling in a bimorph. In 1991, Smits *et al*. developed the linear constituent relations of a cantilever bimorph for static case [14]. Their paper was a milestone in characterizing the electromechanical properties of bending bimorph. In their work, the bimorph was put in a constant electrical field. One end of the bimorph was fixed, the other end was free and subjected to different kind of load (moment, force, or uniformly distributed pressure). Using the internal energy method by assuming thermodynamic quasi-equilibrium, the cantilever bimorph under various constant mechanical/electrical loads was characterized by a four by four matrix equation.

In order to get a better understanding of the bimorph behavior as a function of frequency, Smits *et al*. developed a dynamic admittance matrix for cantilever bimorph which related the harmonically varying diving parameters to their response parameters [15-16]. Through evaluating the dynamic performance of the bimorph under external excitations, the elements in the dynamic admittance matrix were identified analytically. It should be noted that Smits and other researchers only studied bimorphs with one end permanently fixed (clamped) and one end free. While, for a bimorph accelerometer, one end of the bimorph is free and the other end is moving. This is though common condition for bending sensors, it has been seldom studied.

As piezoelectric bimorphs are widely used in industrial equipment, researchers tried to cast the bimorph constituent equations in network representation [17]. In this way, bimorph sensors or actuators can be fully and rapidly incorporated into the world of electronics. Cho *et al.* proposed an important equivalent circuit model in 2000 [18]. In their studies, a 5x5 impedance matrix was determined to describe the dynamic behavior of a bimorph beam. The extensive parameters considered are forces and moments at both ends of the bimorph and electrical voltage across the bimorph. Cho's model is feasible for bimorphs with various end conditions. However, like other equivalent circuit models, Cho's model is complex. For different end conditions or external mechanical loads, complicated circuits have to be developed and then simplified to get the results.

In this paper, a bimorph-based accelerometer is developed to measure linear acceleration at a point of elastic structures. Both an analytical and a numerical model are developed and the results are compared. Using the analytical model, the effects of device geometry and material properties on the dynamic performance of the accelerometer like working frequency range is evaluated. The results of this analysis can be used as a base for mini-accelerometer design and performance optimization.

2. Working Principles of the Accelerometer

The Bimorph Accelerometer contains two series type bimorphs, an insulating layer and a rigid supporting block, as shown in Fig. 1. The two bimorphs have identical geometric and material characteristics and are symmetrically attached to the Glass Epoxide layer, which effectively prevents the charge convection between the left and right bimorphs. The bottom of the insulating layer is tightly glued to the supporting block, which is made of Aluminum and has a dimension of 15 mm x 15 mm x 15.8 mm. As illustrated in Fig. 1, *x* axis is along the bimorph length direction, *y* axis along the bimorph width direction and *z* axis along the thickness direction. The accelerometer is designed to sense the vertical acceleration in *z* direction.

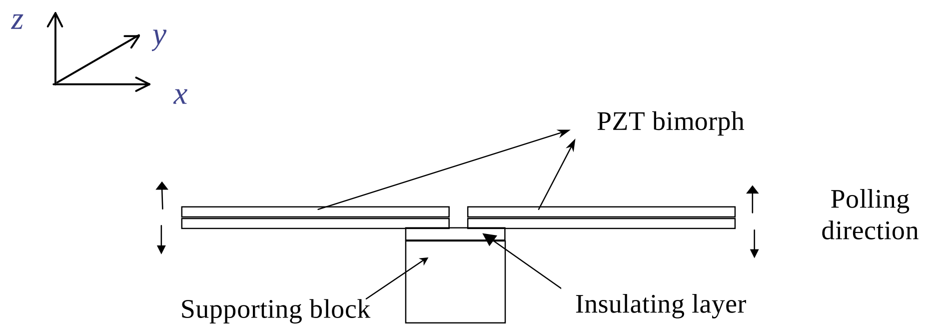

Fig. 1. Structure of the Bimorph Accelerometer.

As illustrated in Fig. 2(a), when translational motion applies to the input port of the transducer, the bimorphs bend upward and downward in same directions. The bending of each bimorph places one PZT layer of the bimorph in tension and the other PZT in compression. As a result of the induced stresses, the bimorph generates an electrical output signal due to the direct piezoelectric effect.

As the transducer is strictly symmetric, for a pure linear acceleration input, the output voltages or charges from the two bimorphs have the same amplitudes and directions. However, in real world, most structures are multi-DOF system and the motion at a measurement point of the accelerometer is often complicated. The translational motion is usually accompanied by rotational motion, as shown in Fig. 2(b). Due to the configuration of the transducer, it is only sensitive to motions in two Degrees of Freedom (DOFs): one translational DOF along *z* direction and one rotational DOF about *y* axis. Owing to the electromechanical interaction between the structure and the sensor, the translation motion results in the identical bending vibrations of the bimorphs and identical voltage output (E_{left_trans} and E_{right_trans}); while the rotation response introduces the out-of-phase bending of the bimorphs and then opposite voltage (E_{left_rot} and E_{right_rot}).

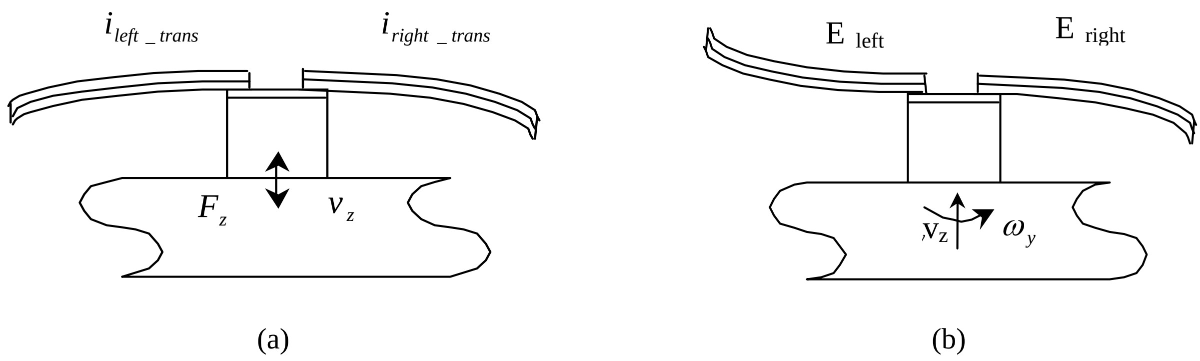

Fig. 2. Working principles of the Bimorph Accelerometer.

The electrical voltages on the left and right bimorphs caused by the vibrations of the structure are therefore:

$$E_{left} = E_{left\_trans} + E_{left\_rot} \tag{1}$$

$$E_{right} = E_{right\_trans} + E_{right\_rot} \tag{2}$$

Owing to the symmetric structure of the sensor, we have:

$$E_{left\_trans} = E_{right\_trans} \tag{3}$$

$$E_{left\_rot} = -E_{right\_rot} \tag{4}$$

Thus the sum of the voltages on the bimorphs becomes

$$E_{left} + E_{right} = 2E_{left\_trans}, \tag{5}$$

where E_{left} (E_{right}) is the output voltage on the left (right) bimorph caused by the translational motion of the structure.

From the above discussions, it can be seen that the information on the translational vibration at the measurement point is embedded in the sum of the output voltage from the bimorphs. It can also be seen that the measurement is independent of the rotational motion at the point, which means that the rotational DOF is successfully decoupled from the translational measurement.

3. Equation of Motion of the Bimorph in the Accelerometer

According to piezoelectric constitutive equations, the electromechanical coupling of the bimorph in Fig. 1 can be expressed as:
For upper PZT:

$$S_1^p = s_{11}^E T_1^p - d_{31} E_3 \tag{6}$$

$$D_3 = -d_{31} T_1^p + \varepsilon_{33}^T E_3 \tag{7}$$

For lower PZT:

$$S_1^p = s_{11}^E T_1^p + d_{31} E_3 \tag{8}$$

$$D_3 = d_{31} T_1^p + \varepsilon_{33}^T E_3 \ , \tag{9}$$

where S_1^p and T_1^p are the strain and stress of the PZT layers parallel with x axis, E_3 and D_3 are the electric field and dielectric displacement along z direction, s_{11}^E is the mechanical compliance under constant electric field condition, d_{31} is the piezoelectric constant, and ε_{33}^T is the permitivity under constant stress condition.

If the bimorph is open-circuited, the electrical displacement D_3 in Eqs. (7) and (9) is zero. Under this condition, for both upper and lower PZT layers in a bimorph, the stress can be expressed as:

$$T_1^p = \frac{s_{11}^E \varepsilon_{33}^T - d_{31}{}^2}{\varepsilon_{33}^T} S_1^p \tag{10}$$

For the middle metal layer sandwiched between the PZT layers, from Hook's Law, we have

$$T_1^m = \frac{S_1^m}{s_{11}^m} , \tag{11}$$

where T_1^m and s_{11}^m are the stress and strain of the metal layer perpendicular to the cross section, s_{11}^m is the mechanical compliance of the metal.

Assuming the bimorph undergoes small defections in the linearly elastic region and the rotary inertia of the bimorph is small, the bimorphs in the accelerometer can be viewed as Euler-Bernoulli beams. Fig. 3 depicts a small bimorph element. In this figure, w is the out-of-plane displacement of the bimorph's neutral plane from its unloaded position to its loaded position. It is usually accompanied by a rotation of the neutral plane as well as a rotation of the beam's cross section. The rotation angle α can be written in terms of the transverse displacement by:

$$u^p = \alpha \cdot z^p \tag{12}$$

$$u^m = \alpha \cdot z^m , \tag{13}$$

where z^p and z^m are vertical coordinate of the PZT layer and the metal layer.

For Euler beams, strains S_1^p and S_1^m are related to the bimorph's displacement w by:

$$S_1^p = \frac{d\alpha}{dx} \cdot z^p = -\frac{d^2 w}{dx^2} \cdot z^p \tag{14}$$

$$S_1^m = \frac{d\alpha}{dx} \cdot z^m = -\frac{d^2 w}{dx^2} \cdot z^m \tag{15}$$

For the bimorph element in Fig. 3, stresses T_1^p and T_1^m create moments about the neutral plane. Summing these moments over the cross-section area results in a total bending moment:

$$M_y = \int\int z^p T_1^p dydz + \int\int z^m T_1^m dydz, \tag{16}$$

where y is the coordinate along bimorph width direction.

Summing the shear stresses T_3^p and T_3^m, the total shear force becomes:

$$F_z = F_z^p + F_z^m = \int\int T_3^p dydz + \int\int T_3^m dydz \tag{17}$$

Consider moment equilibrium of the bimorph element, we have:

$$F_z = \frac{dM_y}{dx} \tag{18}$$

From Eqs. (6) to (9), we have the relationship of stress, strain and electrical field for the upper and lower PZT layers:

$$T_1^p = -\frac{z^p}{s_{11}^E - \frac{d_{31}^2}{\varepsilon_{33}^T}} \cdot \frac{d^2 w}{dx^2} \tag{19}$$

Substituting Eq. (19) into Eqs. (16) and (17), we have

$$M_y = -\frac{2b\varepsilon_{33}^T h_p^3}{3(s_{11}^E \varepsilon_{33}^T - d_{31}^2)} \cdot \frac{d^2 w}{dx^2} = A \cdot \frac{d^2 w}{dx^2} \tag{20}$$

$$F_z = \frac{dM}{dx} = A \cdot \frac{d^3 w}{dx^3}, \tag{21}$$

where

$$A = -\frac{2b\varepsilon_{33}^T h_p^3}{3(s_{11}^E \varepsilon_{33}^T - d_{31}^2)} \tag{22}$$

b = width of the bimorph
h_p = thickness of one PZT layer
$2h_m$ = thickness of middle metal layer

Since the PZT layer in the bimorph has uniform thickness which is hundreds of times smaller than its length and width, significant fringe effects are assumed to be prevented. The electrical field resulted from the excitation therefore becomes:

$$E_3 = \frac{V}{h_p} \tag{23}$$

Applying Newton's second law to the bimorph element in *z* direction yields the following equation which governs the transverse motion of the bimorph:

$$A \cdot \frac{\partial^4 w}{\partial x^4} + 2b(\rho_m h_m + \rho_p h_p) \cdot \frac{\partial^2 w}{\partial t^2} = 0 \tag{24}$$

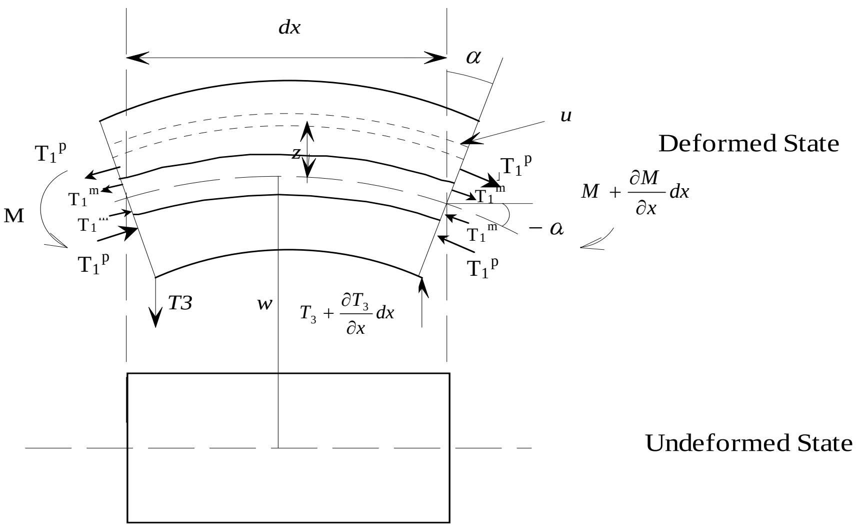

Fig. 3. Diagram of a small bimorph element.

4. Analytical Calibration of the Accelerometer

In this section, the relationship between the input acceleration and the output voltage of the proposed accelerometer will be developed.

As shown in Eq. (24), the out-of-plane displacement *w* is a function of both *x* coordinate and time. Through separating variables, the general solution for harmonic vibration of a bimorph can be expressed as:

$$w = [k_1 \cos(\Omega x) + k_2 \sin(\Omega x) + k_3 \cosh(\Omega x) + k_4 \sinh(\Omega x)] \cdot e^{j\omega t} \tag{25}$$

where

$$\Omega = \sqrt[4]{\frac{b(\rho_p h_p + \rho_m h_m)\omega^2}{-A}} .$$

From Eq. (25), we have:

$$\frac{dw}{dx} = -\alpha = \Omega[-k_1 \sin(\Omega x) + k_2 \cos(\Omega x) + k_3 \sinh(\Omega x) + k_4 \cosh(\Omega x)] \tag{26}$$

$$M_y = A\Omega^2[-k_1 \cos(\Omega x) - k_2 \sin(\Omega x) + k_3 \cosh(\Omega x) + k_4 \sinh(\Omega x)] \tag{27}$$

$$F_z = -A\Omega^3[k_1 \sin(\Omega x) - k_2 \cos(\Omega x) + k_3 \sinh(\Omega x) + k_4 \cosh(\Omega x)] \tag{28}$$

Now we have expressions for displacement, rotation, bending moment and vertical force, which are functions of frequency and the four coefficients k_1, k_2, k_3, k_4. If the boundary conditions of the bimorph are known, the four coefficients can be evaluated. Consequently, the translational and rotational motion as well as moment and force at any point on the bimorph can be easily calculated.

For the accelerometer proposed, as shown in Fig. 4, the left end of the bimorph is mechanically free. The right end is applied with a vertical acceleration input. The above boundary conditions lead to:

$$u_{3A} = d \tag{29}$$

$$\omega_{yA} = 0 \tag{30}$$

$$F_{3B} = 0 \tag{31}$$

$$M_{yB} = 0 \tag{32}$$

Solving Eq. (29) to (32),

$$k_1 = \frac{1 + \cos(\Omega l)\cosh(\Omega l) - \sin(\Omega l)\sinh(\Omega l)}{2[1 + \cos(\Omega l)\cosh(\Omega l)]} \cdot d \tag{33}$$

$$k_2 = \frac{\cos(\Omega l)\sinh(\Omega l) + \cosh(\Omega l)\sin(\Omega l)}{2[1 + \cos(\Omega l)\cosh(\Omega l)]} \cdot d \tag{34}$$

$$k_3 = \frac{1 + \cos(\Omega l)\cosh(\Omega l) + \sin(\Omega l)\sinh(\Omega l)}{2[1 + \cos(\Omega l)\cosh(\Omega l)]} \cdot d \tag{35}$$

$$k_4 = -\frac{\cos(\Omega l)\sinh(\Omega l) + \cosh(\Omega l)\sin(\Omega l)}{2[1 + \cos(\Omega l)\cosh(\Omega l)]} \cdot d \tag{36}$$

From Eqs. (7) and (9), we have the expression for the output voltage:

$$V = -\frac{{h_p}^2 d_{31}\Omega}{2l(\varepsilon_{33}^T s_{11}^E - d_{31}^2)} \cdot [-k_1 \sin(\Omega l) + k_2 \cos(\Omega l) + k_3 \sinh(\Omega l) + k_4 \cosh(\Omega l) - k_2 - k_4] \tag{37}$$

The calibration function of the accelerometer becomes:

$$T = \frac{V}{acceleration} = \frac{V}{-4\pi^2 f^2 \cdot d} \tag{38}$$

$$T = \frac{{h_p}^2 d_{31}\Omega \cdot [-k_1 \sin(\Omega l) + k_2 \cos(\Omega l) + k_3 \sinh(\Omega l) + k_4 \cosh(\Omega l) - k_2 - k_4}{8\pi^2 f^2 l(\varepsilon_{33}^T s_{11}^E - d_{31}^2)[k_1 \cos(\Omega x) + k_2 \sin(\Omega x) + k_3 \cosh(\Omega x) + k_4 \sinh(\Omega x)]} \tag{39}$$

From Equations (37), we can see that the output voltage is a frequency spectrum fully determined by the input motion, the dimensions and material parameters of the bimorph. When the physical properties of the bimorphs are known, the relationship between the input acceleration and output voltage is easily calculated to calibrate the sensor as shown in Equation (39). After the calibration function *T* is obtained, the proposed accelerometer can be used to get the acceleration at its attachment point from the measured output voltage.

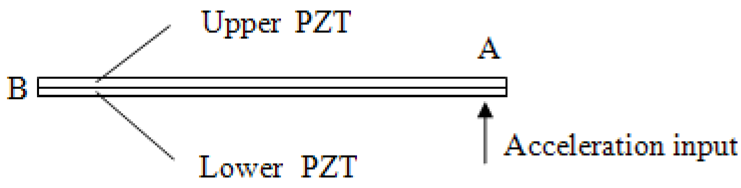

Fig. 4. Bimorph Accelerometer under acceleration input.

5. Numerical Verifications

In this section, first the calibration function *T* of the accelerometer in Equation (38) will be numerically identified. After calibration, to verify the effectiveness of the accelerometer, it will be utilized to detect linear accelerations of one-dimensional beam and two-dimensional plate structures.

5.1. Numerical Calibration

In ANSYS, the piezoelectric elements in the bimorphs are modeled with 3-D Coupled-Field Solid Element SOLID5, which handles the electromechanical coupling taken place in PZT patch by calculating the appropriate element matrix. For the middle metal layer sandwiched between the upper and lower PZT layers in a bimorph, since its length and width are hundreds of times larger than its thickness, solid elements are not suitable in modeling as that will produce huge element numbers and consequently long calculation time. In order to achieve both accurate simulation and short calculation time, Structural Elastic Four Node Shell Element, SHELL 63, is chosen as the modeling element. To model the supporting block and the insulating layer, SOLID 73, which is widely used for three-dimensional modeling of solid structures, is employed. The FEM model of the transducer is shown in Fig. 5.

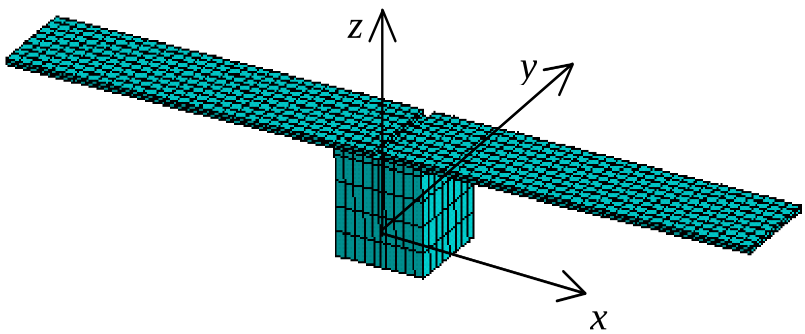

Fig. 5. FEM model of the transducer.

After constructing the FEM model, a sinusoidal acceleration is applied to the input port of the sensor, namely, the bottom of the supporting block. Harmonic response analysis, a technique to determine the steady-state response of a linear structure to sinusoidally varying loads, is then carried out. In Fig. 6, a comparison is made between the analytically and numerically calculated calibration function. It can be seen that the two curves match with each other, which means that the closed form analytical formula is quite accurate in predicting the dynamic performance of the transducer. However, since damping is not included in the analytical solution, as expected, amplitude of T from analytical formula at resonances are larger than that from simulation in which damping effect is considered. It should also be noted that the resonances obtained from analytical formula is bigger than those from simulation. This is because that in analytical derivation the supporting block of the accelerometer, which connects the bimorphs to the tested structure, is not included as in FEM. The existence of the supporting block lowers the resonances in numerical studies.

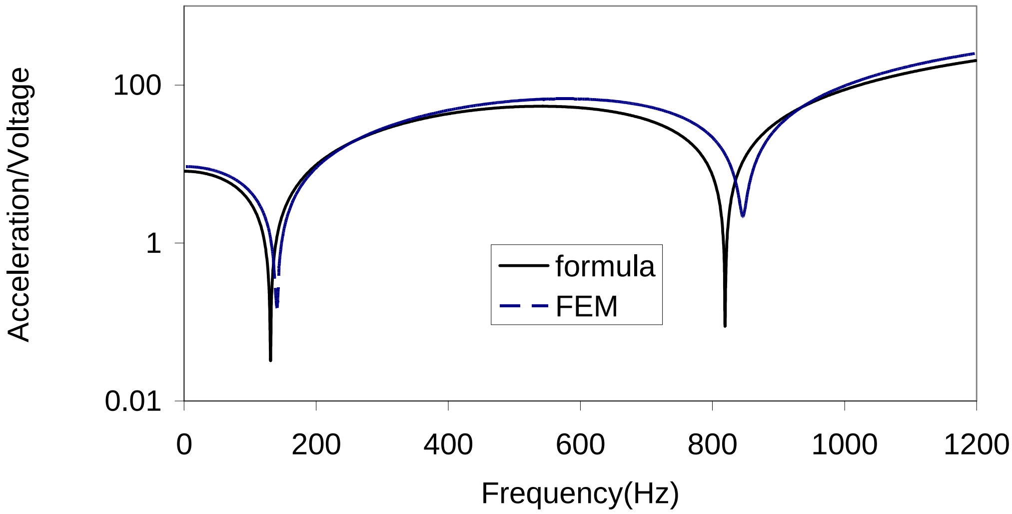

Fig. 6. Comparison of numerically and analytically obtained calibration function.

5.2. Acceleration Measurement Using the Proposed Accelerometer

5.2.1. One-dimensional Beam

A beam clamped at both ends is chosen as the first test structure to study the effectiveness of the proposed accelerometer. The beam is made of Aluminum and is 700 mm in length, 50 mm in width and 3mm in thickness. Two Degrees of Freedom (DOFs) are sufficient to describe the vibrations at any point of the beam: one translational and one rotational. According to Euler-Bernoulli beam theory, there is cross coupling between the two DOFs for all points except the middle point due to the existence of non-zero cross-mobilites [19]. To thoroughly investigate the feasibility of the sensor, here the acceleration at two points is examined: the middle point and the point at 250 mm to the left end of the beam. Finite element models of the transducer & beam system corresponding to the two measurement points are depicted in Fig. 7. After a sinusoidal force with amplitude of 1 Newton is supplied to the beam, which setting the beam into vibration, the output voltages of the two bimorphs are calculated via harmonic analysis. The acceleration input to the accelerometer is also obtained from the analysis via recording the displacement at the attachment point. Now, for each point, we have two set acceleration data determined through two numerical ways. One set is assessed via the new sensor ($a = TV_{out}$); the other set is directly obtained ($a = -4\pi^2 f^2 \cdot uz$). As shown in Fig. 8, they coincide with each other very well in the whole frequency range, even for the 200mm point where the cross coupling between the translational and the rotational DOFs is considerable. It is therefore concluded that the newly developed accelerometer is effective and accurate in measuring acceleration of 1-D beam structure, no matter the cross coupling between different DOFs is zero or not.

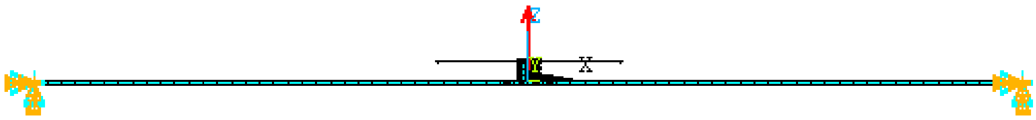

(a) middle point.

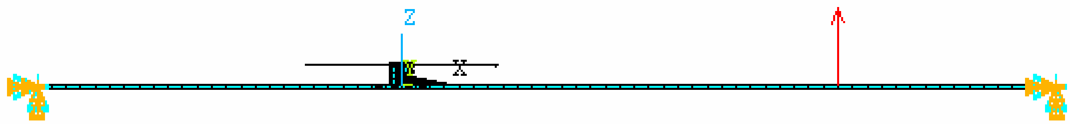

(b) 250 mm point.

Fig. 7. FEM models of the beam and the accelerometer.

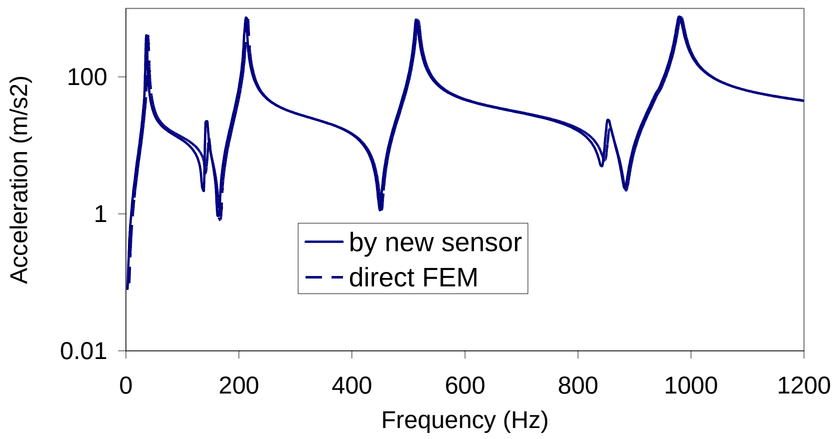

(a) middle point

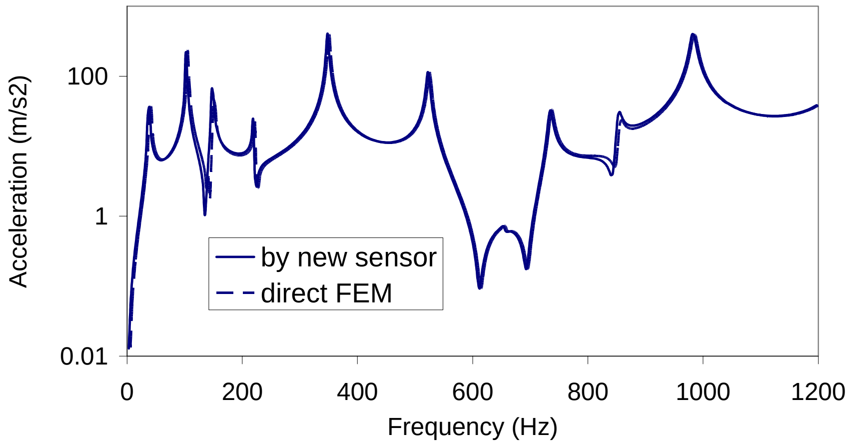

(b) 250 mm point

Fig. 8. Comparison of the linear acceleration between (1) numerical data obtained by the new sensor; (3) numerical data directly obtained from the beam model (without accelerometer).

5.2.2. Two-dimensional Plate

A two-dimensional plate is utilized as another test structure to further investigate the effectiveness of the new transducer in measuring acceleration. The aluminum plate is clamped with two adjacent edges, having dimensions of 700 mm x 500 mm x 3 mm. Any point on the plate has three active Degrees of Freedom: translational along *z* axis (*uz*), rotation about *x* axis (*rotx*), and rotation about *y* axis (*roty*). The FEM model of the sensor & plate system is depicted in Fig. 9.

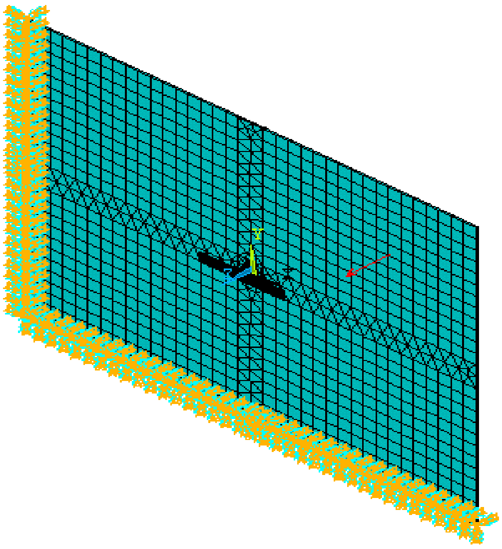

Fig. 9. FEM model of the plate and the sensor.

Following a similar procedure as for the beam case, the output voltage of the bimorphs is obtained and the acceleration at the attachment point is then calculated ($a = TV_{out}$). The acceleration is also calculated from a plate model without bimorph accelerometer attached to check the accuracy of the acceleration detected by the accelerometer. It can be observed from Fig. 10 that even vibrations in three directions simultaneously exist at the measurement point (center point), the linear acceleration in the desired direction (*uz*) can be accurately detected by the prototype sensor. It is therefore concluded that the accelerometer is also effective in measuring linear acceleration of two-dimensional structure.

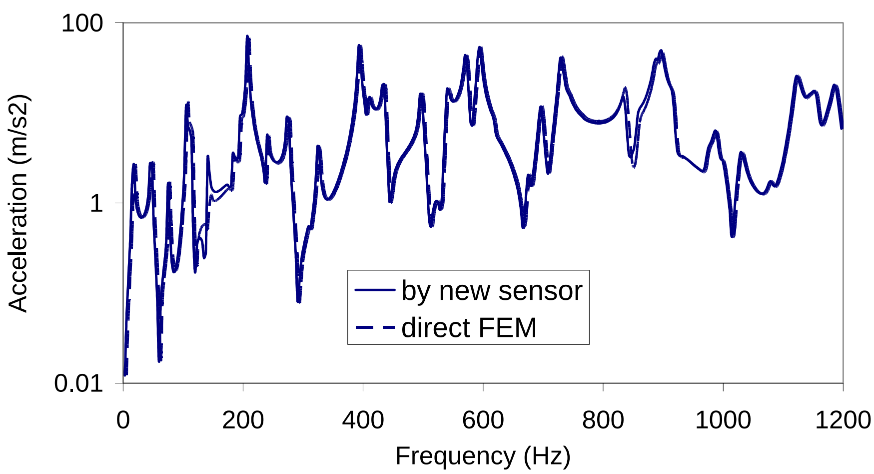

Fig. 10. Comparison of acceleration over output voltage.

6. Optimization of the Accelerometer

Generally, for a sensor, its working frequency range better avoids its resonances so that in real experiments the measurement errors around the resonances can be minimized. As shown in Fig. 6, the prototype sensor only has smooth response in the frequency range from 200 Hz to 800 Hz. In addition, a sensor is desired to be as small as possible to reduce its loading effect.

In Section IV, the closed-form calibration function of the proposed accelerometer has been analytically derived. Taking advantages of this formula, it is possible to improve the sensing performance of the proposed prototype accelerometer in wider frequency range through revising its essential design parameters.

The analytical formula in Eq. (39) is derived base on beam theory. According to beam theory, the beam (bimorph) length and thickness have great effect on the resonant frequencies of the accelerometer. Here the cantilevered length of the bimorph is adjusted to change the resonances. To maintain a beam shape, the width is changed to 2.8 mm. The thickness and material properties of the bimorphs remain unchanged. As illustrated in Fig. 11, the optimized accelerometer has a quite smooth response from 100 Hz to 12 000 Hz, which greatly improve the sensing frequency range of the transducer.

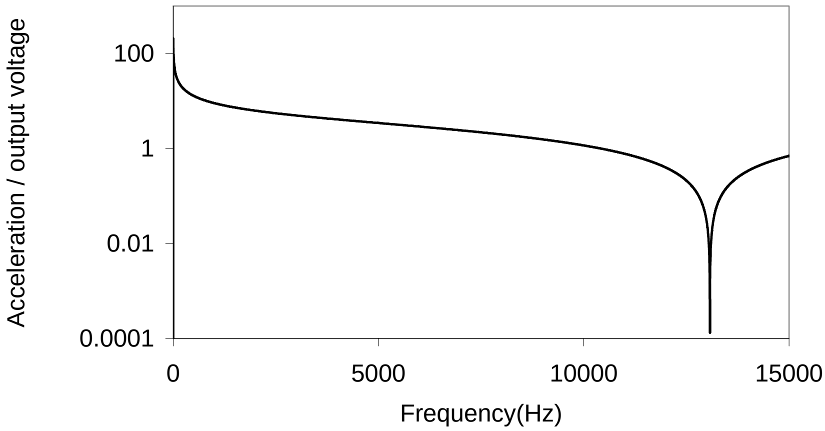

Fig. 11. Calibration function of optimized accelerometer.

7. Conclusions

In this paper, an analytical model for a bimorph accelerometer with symmetric bending bimorphs is developed. The model takes into account the effect of device geometry and material properties, and agrees well with the results obtained by the finite element analysis. In addition, it is found that with appropriate geometrical dimensions, wide measurement frequency range can be achieved. The results of this study can be readily applied to mini- or micro accelerometer design and its structural optimization.

Reference

[1]. I. Takuro, Fundamentals of piezoelectricity, *Oxford University Press*, Oxford, New York, 1990.
[2]. J. V. Randeraat and R. E. Setterington, Piezoelectric ceramics, *Mullard Limited*, 1974.
[3]. B. JAFFE, W. R. COOK and H. JAFFE, Piezoelectric Ceramics, London, *Academic Press*, UK, 1971.

[4]. Q. M. Wang, X. H. Du, B. Xu and L. E. Cross, Electromechanical coupling and output efficiency of piezoelectric bending actuator, *IEEE Transactions on Ultrasonics, Ferroelectrics, and Frequency Control*, Vol. 46, 3, 1999, pp. 638–646.

[5]. J. J. Shaffer and D. L. Fried, Bender-bimorph scanner analysis, *Applied Optics*, Vol. 9, 4, 1970, pp. 933-937.

[6]. J. K. Lee, Piezoelectric bimorph optical beam scanners: analysis and construction, *Applied Optics*, Vol.18, 4, 1979, pp. 454-459.

[7]. V. D. Kuge, B. Xu, Q. M. Zhang and L. E. Cross, Bimorph-based piezoelectric air acoustic transducer: model, *Sensors and Actuators A*, Vol. 69, 1998, pp. 234-242.

[8]. W. J. Denkmann, R. E. Nickell and D. C. Stickler, Analysis of structural acoustic interactions in metal-ceramic transducers, *IEEE Transactions on Audio and Electroacoustics*, Vol. 21, 4, 1973, pp. 317-324.

[9]. W. J. Spencer, W. T. Corbett, L. R. Dominguez and B. D. Shafer, An electronically controlled piezoelectric insulin pump and valves, *IEEE Transactions on Sonics and Ultrasonics*, Vol. 25, 1978, pp. 153-156.

[10]. O. Kawasaki, T. Nishikura, Y. Imasaka, M. Sumihara, K. Takeda and H. Yoneno, Ultrasonic motors, *IEEE Tokyo Section*, Denshi Tokyo, Vol. 26, 1987, pp. 158-161.

[11]. M. Toda, So. Osaka and E. O. Johnson, A new electromotional device, *RCA Engineer*, Vol. 25, 1, 1979, pp. 24-27.

[12]. B. Bill and A. L. Wicks, Measuring simultaneously translational and angular acceleration with the new translational-angular-piezobeam (TAP) system, in *Proceedings of Transducers' 89, 5th International Conference on Solid-State Sensors and Actuators and Eurosensors III*, Montreaux, Switzerland, 1989, pp. 1229.

[13]. Datasheet of Lateral Accelerometer Type 8840, [online]. Available at: http://www.kistler.com/do.productfinder.sg.en-sg?param=App.8840

[14]. G. Smits, S. I. Dalke and T. K. Cooney, The constituent equations of piezoelectric bimorphs, *Sensors and Actuators A*, Vol. 28, 1991, pp. 41–61.

[15]. Jan G. Smits and Arthur Ballato, Dynamic admittance matrix of piezoelectric cantilever bimorphs, *Journal of Microelectromechanical Systems*, Vol. 3, 3, 1994, pp. 105-112.

[16]. Jan G. Smits and Arthur Ballato, Dynamic behavior of piezoelectric bimorphs, *IEEE Untrasonics Symposium*, 1993, pp. 463-465.

[17]. Arthur Ballato and Jan G. Smits, Simulation networks of piezobimorphs for robotic actuators, *IEEE Ultrasonics Symposium*, Vol. 3, 1998, pp. 1173-1176.

[18]. Y. S. Cho, Y. E. Park, C. S. Han and S. K. Ha, Five-port equivalent electric circuit of piezoelectric bimorph beam, *Sensors and Actuators A*, Vol. 84, 2000, pp. 140–148.

[19]. J. Su and B. M. Gibbs, Measurement of point moment mobility in the presence of non-zero cross mobility, *Applied Acoustics*, Vol. 54, 1, 1998, pp. 9-26.

___

Guide for Contributors

Aims and Scope

Sensors & Transducers Journal (ISSN 1726-5479) provides an advanced forum for the science and technology of physical, chemical sensors and biosensors. It publishes state-of-the-art reviews, regular research and application specific papers, short notes, letters to Editor and sensors related books reviews as well as academic, practical and commercial information of interest to its readership. Because it is an open access, peer review international journal, papers rapidly published in *Sensors & Transducers Journal* will receive a very high publicity. The journal is published monthly as twelve issues per annual by International Frequency Association (IFSA). In additional, some special sponsored and conference issues published annually.

Topics Covered

Contributions are invited on all aspects of research, development and application of the science and technology of sensors, transducers and sensor instrumentations. Topics include, but are not restricted to:

- Physical, chemical and biosensors;
- Digital, frequency, period, duty-cycle, time interval, PWM, pulse number output sensors and transducers;
- Theory, principles, effects, design, standardization and modeling;
- Smart sensors and systems;
- Sensor instrumentation;
- Virtual instruments;
- Sensors interfaces, buses and networks;
- Signal processing;
- Frequency (period, duty-cycle)-to-digital converters, ADC;
- Technologies and materials;
- Nanosensors;
- Microsystems;
- Applications.

Submission of papers

Articles should be written in English. Authors are invited to submit by e-mail editor@sensorsportal.com 6-14 pages article (including abstract, illustrations (color or grayscale), photos and references) in both: MS Word (doc) and Acrobat (pdf) formats. Detailed preparation instructions, paper example and template of manuscript are available from the journal's webpage: http://www.sensorsportal.com/HTML/DIGEST/Submition.htm Authors must follow the instructions strictly when submitting their manuscripts.

Advertising Information

Advertising orders and enquires may be sent to sales@sensorsportal.com Please download also our media kit: http://www.sensorsportal.com/DOWNLOADS/Media_Kit_2008.pdf